# Induced 3d and 4f magnetism in $Gd_{1-x}Pr_xNi_2$ Laves phase alloys



2008 J. Phys.: Condens. Matter 20 025218

(http://iopscience.iop.org/0953-8984/20/2/025218)

J. Phys.: Condens. Matter **20** (2008) 025218 (6pp) doi:10.1088/0953-8984/20/02/025218

# Induced 3d and 4f magnetism in $Gd_{1-x}Pr_xNi_2$ Laves phase alloys

**K Bouziane[1,3], C Carboni[1] and C Morrison[2]**

[1] Department of Physics, College of Science, Sultan Qaboos University, PO Box 36, Al-Khodh 123, Sultanate of Oman
[2] School of Physics and Astronomy, University of Southampton, Highfield, Southampton SO17 1BJ, UK

E-mail: bouzi@squ.edu.om

Received 22 August 2007, in final form 15 November 2007
Published 13 December 2007
Online at stacks.iop.org/JPhysCM/20/025218

**Abstract**

The series of $Gd_{1-x}Pr_xNi_2$ ($x = 0.25$, 0.40, and 0.60) polycrystalline samples has been investigated using x-ray diffraction and magnetometry. The x-ray diffraction measurements showed that the lattice constant and the relative intensities of the C15 superstructure $I_{511}/I_{440}$ and $I_{511}/I_{220}$ increase with the praseodymium content, reflecting an increasing number of ordered vacancies at the 4a sites. The temperature dependences of the zero-field cooled ($M_{ZFC}(T)$) and field cooled ($M_{FC}(T)$) magnetizations show that a moment is induced by the gadolinium on the $Pr^{3+}$ ion and on the nickel subsystem. In the ordered phase both induced moments are antiparallel to that of the $Gd^{3+}$ ion. A cusp is observed at a temperature $T_{max}$ in the $M_{ZFC}(T)$ curve. Both critical temperatures $T_c$ and $T_{max}$ are found to decrease with increasing praseodymium content, indicating a reduction in strength of the antiparallel coupling for Gd–Pr and Gd–Ni pairs.

(Some figures in this article are in colour only in the electronic version)

## 1. Introduction

The $RT_2$ alloys where R is a rare-earth element and T is a transition metal are probably the simplest kinds of rare-earth intermetallic compounds. Apart from a few exceptions they crystallize in the cubic $MgCu_2$ structure, space group $Fd3m$. The R ion sits at a site of cubic symmetry surrounded by twelve T ions as nearest neighbours and four R ions as second-nearest neighbours. The site symmetry of the $T$ ion is tetragonal. There are eight formula units per unit cell. The ordered sublattice of vacancies at the R sites give rise to a C15 superstructure. In spite of extensive study for more than three decades, the binary $RT_2$ and the pseudo-binary ($RT_2R'T'_2$) compounds continue to attract the interest of many researchers. The $RNi_2$ series is particularly interesting; there is still some confusion regarding the contribution of the nickel to the magnetization. Values between 0 and 0.26 $\mu_B$ for the magnitude of the magnetic moment of the nickel in $GdNi_2$ have been reported [1–3] in the literature. More recently, magnetic x-ray circular dichroism measurements on $GdNi_2$ have given respectively 0.14 and 0.06 $\mu_B$ for the spin and orbital contributions to the induced moment on nickel [4]. It is generally accepted that in Gd–Ni intermetallic alloys with low gadolinium content, the induced itinerant magnetic moment on Ni couples antiparallel to the localized moment of the $Gd^{3+}$ ion. The magnitude of the moment on nickel increases with the gadolinium content. The nickel's moment is 0.16 $\mu_B$ in $GdNi_5$ [5] and as already mentioned of the order of 0.26 $\mu_B$ for $GdNi_2$ [3, 6–8]. In alloys with high gadolinium content, the moment on nickel is much larger ($\mu_{Ni} \sim 0.6\ \mu_B$ in GdNi) and couples ferromagnetically to the gadolinium moment [9, 10]. The type of magnetic order and the induced magnetic moment on nickel remain open questions. The magnetic moment on nickel has been attributed either to a charge transfer resulting in a complete filling of the 3d band or to the effective field of the gadolinium sublattice. Recent specific heat measurements on $GdNi_2$ indicate spin fluctuations induced by f–d exchange in the 3d electron subsystem of nickel [11].

It has also been reported that the $RNi_2$ compounds with R = Tb, Gd, Sm and Y undergo both temperature-induced [12] and pressure-induced [13] order–disorder transitions in the superlattice of vacancies. In particular $GdNi_2$ displays a sharp pressure-induced order–disorder transition centred at about 9 GPa [13].

[3] Author to whom any correspondence should be addressed.

 

The present work is an investigation of the series $Gd_xPr_{1-x}Ni_2$ ($x = 0.25, 0.40, 0.60$). The motivation for this work was to gain a better understanding of the terminal compounds $GdNi_2$ and $PrNi_2$. In $GdNi_2$ the $Gd^{3+}$ ion (S state) does not experience any crystal field interaction and retains the fully polarized free-ion moment $\mu_{Gd} = 7\ \mu_B$ in the material. The compound displays magnetic order below 75 K [14, 15]. The ordering is driven by the exchange interaction between the rare-earth ions via the conduction electrons. The ordering of the gadolinium moments then induces a polarization on the nickel. In $PrNi_2$ the ground manifold of the $Pr^{3+}$ ion ($J = 4$) is split by the crystal field interaction, and the ground state is a non-magnetic $\Gamma_3$ doublet; the material remains a van Vleck paramagnet at temperatures as low as 12 mK [14, 16]. In the $Gd_xPr_{1-x}Ni_2$ series the $\Gamma_3$ ground state of the $Pr^{3+}$ ion is split by the local field created by the ordered $Gd^{3+}$ ions and a magnetic moment is thus induced on the $Pr^{3+}$ ions. The coupling of the moment on the praseodymium to the moments on the gadolinium and the nickel as well as the evolution of the magnitude of the moments as a function of composition are the objects of the present work.

This paper is organized as follows. In section 3, we describe our computation approach based on the Weiss mean-field theory. The structural properties are presented in section 4.1, followed by a description and a discussion of the experimental magnetic and computation results in section 4.2. Finally, a conclusion is drawn based on the above results in section 5.

## 2. Experimental details

The compounds of composition $Gd_{1-x}Pr_xNi_2$ alloys ($x = 0.25$, 0.40, and 0.60) were prepared at the University of Manchester (UK) by melting the constituents (3N purity for the rare-earth elements and 4N for nickel) in an arc furnace under an atmosphere of purified argon. The starting materials contained a 2% excess of praseodymium to compensate for the anticipated loss by evaporation. The ingots were turned over and re-melted three times to ensure their homogeneity, then annealed for two weeks at 900 °C and finally crushed to a fine powder sample for the measurements. The structure was investigated at room temperature using powder x-ray diffraction with a Philips PW 1700 diffractometer with Cu K$\alpha$ radiation. The magnetization measurements were carried out by using a vibrating sample magnetometer (VSM) in a magnetic field up to 15 kOe. The field cooling and zero-field cooling magnetization curves were performed with an applied magnetic field $H = 1$ kOe in the temperature range 250–4.2 K. The VSM was calibrated using pure nickel ($M_s = 54.9$ emu g$^{-1}$).

## 3. Computation approach

The magnetic moment on the praseodymium ion $\mu_{Pr}$ is calculated using

$$\mu_{Pr} = g_J \beta \langle J_Z \rangle \tag{1}$$

where $g_J$ is the Landé $g$-factor ($g_J = 0.805$ for $Pr^{3+}$), $\beta$ is the Bohr magneton and $\langle J_Z \rangle$ is the thermal average of the expectation value of the $z$-component of the total angular momentum of the f electrons of the praseodymium ion.

The states of the praseodymium ion in $GdNi_2$ are obtained from the single-ion electronic Hamiltonian

$$\mathcal{H}_{el} = -\boldsymbol{\alpha} \cdot \mathbf{J} + B_4O_4 + B_6O_6 \tag{2}$$

where $B_4$ and $B_6$ are the crystal field parameters in the notation of Lea *et al* [17] and $\boldsymbol{\alpha} = g_J \beta \mathbf{X}$ where $\mathbf{X}$ is the effective exchange field seen by the praseodymium ion in the notation of McMorrow *et al* [18].

Although the substitution of gadolinium by praseodymium causes an observable change in the lattice parameters (see section 4.1), we assume that for the purpose of this work the crystal field parameters can be considered constant across the series. The crystal field parameters $B_4 = -2.02 \times 10^{-2}$ K and $B_6 = -6.96 \times 10^{-4}$ K obtained by Melero *et al* [19] from inelastic neutron scattering on pure $PrNi_2$ were used for the present calculations.

The magnitude of $\boldsymbol{\alpha}$ for the various concentrations of praseodymium was estimated by an *ad hoc* scaling following McMorrow *et al* [18]. For the scaling the Gd–Gd exchange interaction energy $J_{11} = 1.75$ K and the Gd–Ni exchange interaction energy $J_{12} = -3.8$ K given by Yano *et al* [3] for pure $GdNi_2$ have been used.

For completeness we give the ground state ($\Gamma_3$ doublet) of the praseodymium ion in $PrNi_2$ in zero field:

$$\begin{aligned} |E_0\rangle &= 0.707|-2\rangle + 0.707|2\rangle \\ |E_1\rangle &= 0.540|-4\rangle + 0.645|0\rangle + 0.540|4\rangle. \end{aligned} \tag{3}$$

The first excited state ($\Gamma_4$ triplet) is at 40 K.

The computations have shown a significant anisotropy of the praseodymium magnetization. The largest moment is obtained when the ion is magnetized along the $\langle 100 \rangle$ direction, and a reduction of about 20% in the magnitude of the moment is observed when the moment is forced along the $\langle 110 \rangle$ direction.

The magnetic properties (the magnetic moments and exchange coupling) of the series $Gd_{1-x}Pr_xNi_2$ (see section 4.2) are analysed on the light of the above computations.

## 4. Results and discussion

We discuss first the x-ray diffraction data; the magnetization measurements combined with our theoretical computation will be presented and discussed in the next section.

### *4.1. Structural properties*

The powder x-ray diffraction patterns for the three samples of $Gd_{1-x}Pr_xNi_2$ ($x = 0.25$, 0.4 and 0.6) are shown in figure 1. The reflections were indexed to the cubic superstructure of C15. The occupancy at the 4a sites can be assessed from the intensity of the strongest superstructure line (511) relative to the intensity of either (220) or (440) [13]. Figure 2(a) shows the variation of $I_{511}/I_{220}$ and of $I_{511}/I_{440}$ for the different concentrations of praseodymium. It is observed that both relative intensities increase with the praseodymium content;

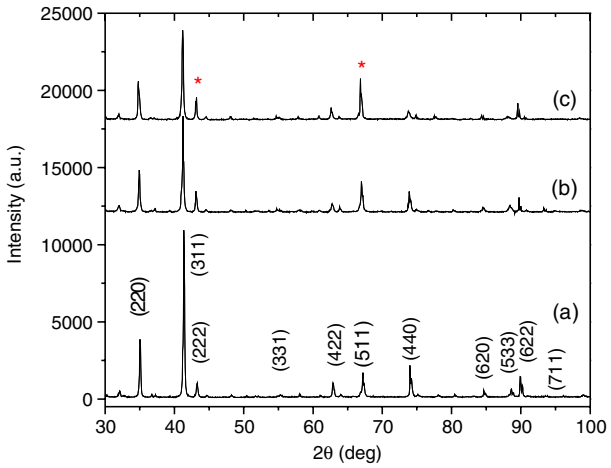


**Figure 1.** Room temperature XRD patterns of the $Gd_{1-x}Pr_xNi_2$ series for (a) $x = 0.25$, (b) $x = 0.40$ and (c) $x = 0.60$. The asterisk symbol (*) indicates the superstructure reflections.

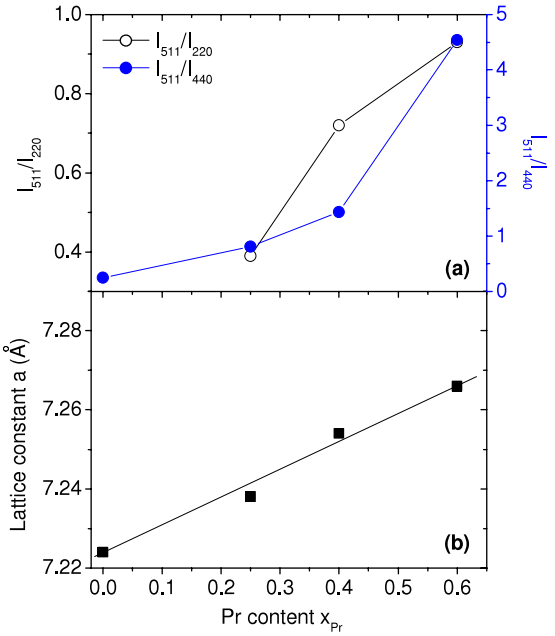


**Figure 2.** The variation of (a) the superstructure relative intensities $I_{511}/I_{220}$ and $I_{511}/I_{440}$, and (b) the lattice constant $a$ for the pseudo-binary $Gd_{1-x}Pr_xNi_2$ alloy as a function of the praseodymium content. The solid lines are guides to the eyes. The $I_{511}/I_{440}$ for $x = 0$ is taken from [13].

this implies that for higher praseodymium concentrations there is an increase in the number of ordered vacancies at the 4a site. This observation is consistent with previous work which showed that the occurrence of vacancies at the 4a sites increases for larger radii of the lanthanide ion ($Pr^{3+}$: 1.266 Å and $Gd^{3+}$: 1.193 Å) [20]. Figure 2(b) shows the variation of the lattice parameter with praseodymium content. As expected the lattice constant increases almost linearly with the praseodymium content. The lattice parameters of the end members $GdNi_2$ and $PrNi_2$ obtained by extrapolation are 7.223 and 7.295 Å respectively.

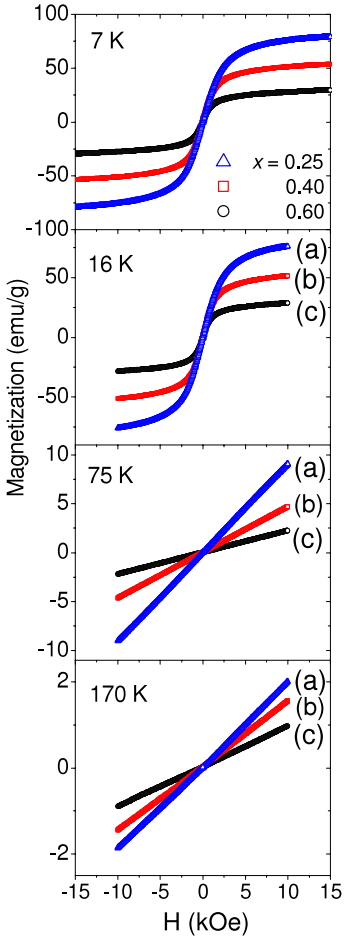


**Figure 3.** The magnetization loops $M(H)$ at representative temperatures between 7 and 170 K for $Gd_{1-x}Pr_xNi_2$ alloys for (a) $x = 0.25$, (b) $x = 0.40$ and (c) $x = 0.60$.

### *4.2. Experimental magnetic and computation results*

The magnetization loops $M(H)$ for the three compounds $Gd_{1-x}Pr_xNi_2$ ($x = 0.25$, 0.40 and 0.60) were obtained at various temperatures between 7 and 170 K. Figure 3 shows representative $M(H)$ curves for the magnetically ordered phase ($T = 7$ and 16 K) and for the paramagnetic phase ($T = 75$ and 170 K). For all the low temperature measurements the samples were cooled in zero field (ZFC). The behaviour at $T = 75$ and 175 K is that of a paramagnet. The susceptibility decreases with the praseodymium content. For all the compounds there is no observable sign of approaching saturation at 10 kOe. In the ordered phase at 7 and 16 K the magnetization has almost reached its saturation value at 15 kOe. The magnetization $M(0)$ at 0 K was determined by extrapolating the graph of $M(H)$ versus $1/H$ to $1/H = 0$. The extrapolation was done with the data obtained at $T = 7$ and 16 K. Because the magnetization is nearly constant as the temperature varies between 7 and 16 K the uncertainty on $M(0)$ is estimated to be less than 5%. The values of $M(0)$ per formula unit thus obtained for the various compositions are given in the sixth column of table 1. However, the data given in table 1 must be treated with some caution as the estimated 5% uncertainty on $M(0)$ does not take into account

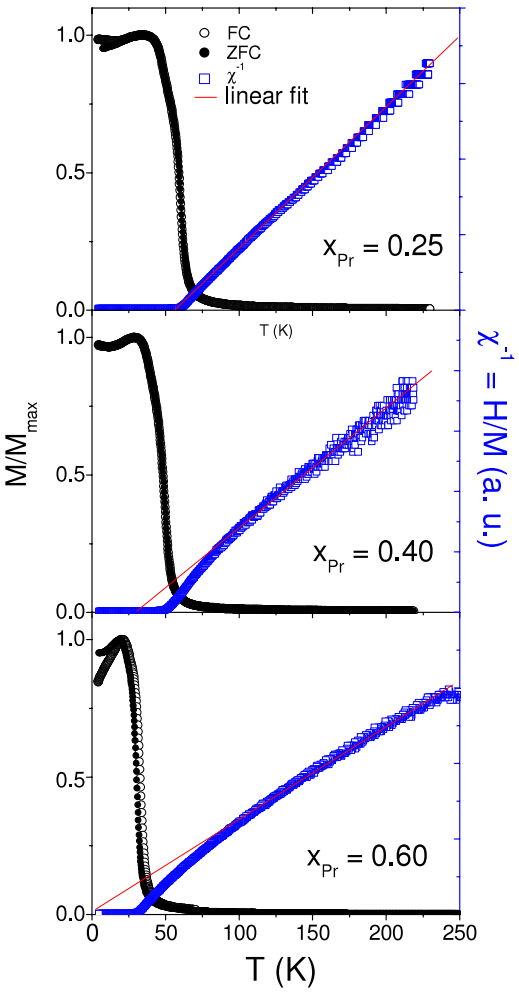


**Figure 4.** The zero-field cooling (ZFC) and field cooling (FC) magnetizations as well as the reciprocal of susceptibility ($H/M$) as a function of temperature at applied field of 1 kOe for the $Gd_{1-x}Pr_xNi_2$ series. The lower curve at low temperature is the ZFC curve.

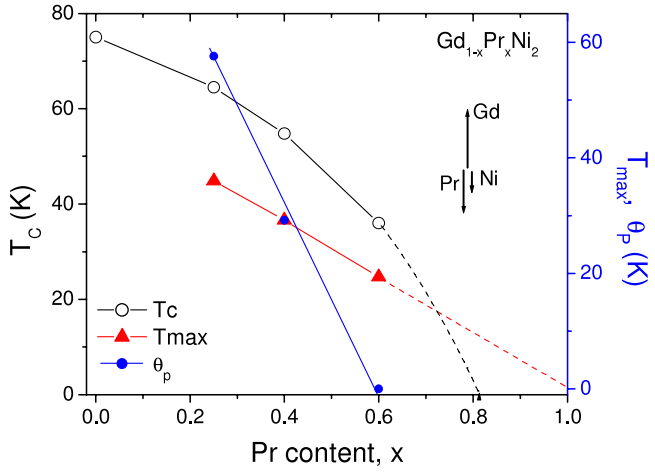


**Figure 5.** The variation of the critical temperatures as a function of praseodymium content: the Curie temperature ($T_c$), the temperature associated with the maximum magnetization ($T_{max}$) and the paramagnetic Curie constant ($\theta_p$) for $Gd_{1-x}Pr_xNi_2$ alloys.

**Table 1.** The values of the relevant magnetic moments in $Gd_{1-x}Pr_xNi_2$. $|\alpha|$ is the magnitude of the effective field seen by the praseodymium ion; $\mu_{Pr}$ is the averaged magnetic moment on the praseodymium ion; $\mu_{Pr}$/fu, and $\mu_{Gd}$/fu are, respectively, the contributions of the praseodymium and the gadolinium to the magnetization per formula unit; $\mu_{Exper}$/fu is the measured magnetization per formula unit; $\mu_{Ni}$/fu is the inferred value of the contribution of the Ni sublattice to the magnetization per formula unit and $\mu_{Ni}$/atom is the corresponding moment per nickel atom.

| $x_{Pr}$ | $\|\alpha\|$ (K) | $\mu_{Pr}$ ($\mu_B$) | $\mu_{Pr}$/fu ($\mu_B$) | $\mu_{Gd}$/fu ($\mu_B$) | $\mu_{exper}$/fu ($\mu_B$) | $\mu_{Ni}$/fu ($\mu_B$) | $\mu_{Ni}$/atom ($\mu_B$) |
|---|---|---|---|---|---|---|---|
| 0 | 45 | — | 0 | 7 | 6.5 | 0.5 | 0.25 |
| 0.25 | 32 | 2.7 | 0.67 | 5.25 | 4.1 | 0.48 | 0.24 |
| 0.40 | 24 | 2.6 | 1.04 | 4.2 | 2.8 | 0.36 | 0.18 |
| 0.60 | 14 | 2.0 | 1.2 | 2.8 | 1.49 | 0.11 | 0.05 |

**Table 2.** The values of $T_c$, $T_{max}$ and the paramagnetic Curie constant $\theta_p$ for the various compounds.

| | $x_{Pr}$ | | | |
|---|---|---|---|---|
| | 0 | 0.25 | 0.40 | 0.60 |
| $T_c$ | 75 | 64.5 | 54.8 | 36 |
| $\theta_p$ | ∼75 | 57.6 | 28.6 | 0 |
| $T_{max}$ | — | 36 | 29.2 | 19.4 |

any possible systematic error from the VSM measurements. Also the anisotropy will cause some systematic reduction in the measured value of the $M(0)$. Finally the uncertainty on the crystal field parameters and the estimated value of $\alpha$ are not known. All these factors will bring about a systematic error on the derived value for the nickel moment; a rough estimation for this uncertainty would be of the order of 60–70%. Therefore, only the trend in the variation of the magnetic moments as a function of concentration should be considered.

The zero-field cooled ($M_{ZFC}$) and field cooled ($M_{FC}$) magnetizations curves as well as the reciprocal of susceptibility ($H/M$) as a function of temperature are shown in figure 4. The ordering temperature, obtained from the graph and reported in table 2, decreases as expected with the praseodymium content. All the $M_{ZFC}(T)$ and $M_{FC}$ curves show a cusp at temperature $T_{max}$. It is observed that $T_{max}$ decreases with the praseodymium content (see table 2). The cusp is most pronounced in $M_{FC}$ for $x_{Pr} = 0.60$. There is little difference between the cusps in $M_{FC}(T)$ and $M_{ZFC}(T)$ for $x_{Pr} = 0.40$ and 0.25.

A careful observation of figure 4 at temperatures below $T_{max}$ shows that at towards the lowest temperatures, the magnetization increases again with decreasing temperature. Further work is required to ascertain whether the existence of this cusp is an intrinsic property of the material or whether it is due to the presence of domains and domain walls. However, at this stage the following observation can be made from the plots in figure 5: the temperature $T_{max}$ decreases linearly with the praseodymium content and the extrapolation indicates that $T_{max}$ will vanish for $PrNi_2$. Also from figure 4 it can be seen that the cusp is progressively less pronounced as the praseodymium content is reduced and would disappear for $GdNi_2$. The increase of the average praseodymium moment due to the depopulation of the excited states at

low temperatures could be responsible for the cusp since the $Pr^{3+}$ moment is coupled antiparallel to that of the $Gd^{3+}$. Also, because the anisotropy of the $Pr^{3+}$ ion increases at low temperatures the gadolinium and the praseodymium moments are no longer collinear with the applied field. This, together with the polycrystalline nature of the specimen, may cause a decrease in the component of the average magnetization measured along the direction of the applied field [21]. Indeed, in a polycrystalline sample the direction of the easy axis varies between individual crystallites. As the system is cooled down, it settles into its lowest energy state. Accordingly, the system will generally have a magnetization for each crystallite that is not perfectly aligned with the field. Measurements of the magnetization component parallel to the applied field with decreasing $T$ will show a drop in magnetization averaged over many crystallites. The difference between ZFC and FC magnetization is similar to the case for the so-called sperimagnets. Finally, a spin glass behaviour should not be totally ruled out at this stage.

The magnitudes and possible coupling of the moments in the material at zero temperature are now presented. The computation of the effective exchange field $\boldsymbol{\alpha}$ and the magnetic moment on the $Pr^{3+}$ ion per formula unit, based on the theory presented in section 3, are displayed in table 1 (columns 2 and 4). The average values of the moment given in table 1 for the praseodymium are an average taking into account the polycrystalline nature of the specimen used for the measurements. For the calculation it has been assumed that the moment of the gadolinium ion is parallel to the small applied magnetic field and that the moments of the praseodymium and the nickel are collinear with the moment of the gadolinium. Due to the anisotropy of the praseodymium, this assumption is not rigorously true since at low fields the easy axis of magnetization is defined by the praseodymium moment. However, this assumption will nevertheless be made as a first approximation for the purpose of the present work.

Column 6 of table 1 gives the measured magnetization per formula unit extrapolated to zero temperature; column 5 gives the average moment per unit formula of $Gd^{3+}$ assuming the ion retains its fully polarized value in all compounds. In fact, in the calculation of the moment on the $Pr^{3+}$ ion any reduction due to the possible intra-ionic 4f–5d hybridization observed by Givord and Courtois [22] in the iron homologue $PrFe_2$ has not been considered. From the data in these three columns (4, 5 and 6) one can deduce the nickel contribution per formula unit if the coupling between the three magnetic moments is known. The values quoted in the last two columns of table 1 was obtained assuming that the three moments are collinear and that the praseodymium and the nickel moments are both antiparallel to the gadolinium moment. Any other collinear arrangement of the moments leads to an unrealistic value for the magnitude of the nickel's moment. The proposed arrangement of the orientation of the moments is also supported by the following argument. The inverse of susceptibility at 1 kOe above the Curie temperature (figure 4) follows closely a Curie–Weiss-like behaviour for the samples with a low concentration of praseodymium whereas the sample with $x_{Pr} = 0.60$ behaves as a Curie-like paramagnet ($\theta_p = 0$).

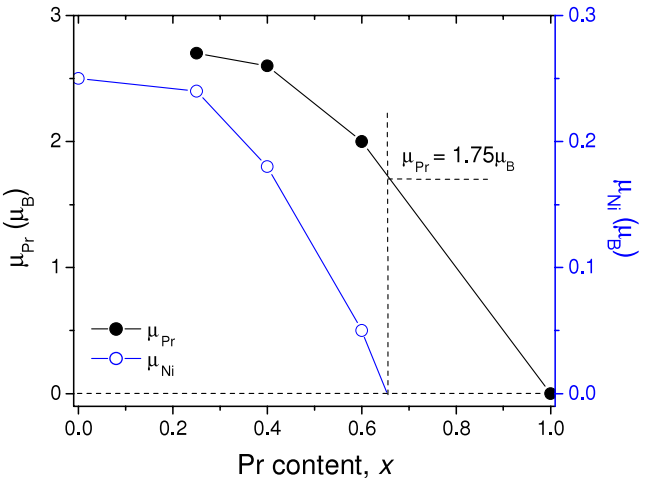


**Figure 6.** The induced magnetic moment on the praseodymium and the nickel as a function of the praseodymium content. The induced magnetic moments on Ni in $GdNi_2$ and $PrNi_2$ are taken from [14] and [3], respectively.

The values of $\theta_p$ do not have the linear relationship with $T_c$ as expected for a ferromagnet, and the deviation from linearity is accentuated when the praseodymium content increases due to crystal field effects. This observation would suggest an enhancement of the antiferromagnetic character in the coupling between the moments in the material.

Figure 6 shows the evolution of the two induced moments as a function of the praseodymium content. Since both the 4f magnetism on praseodymium and the 3d magnetism on nickel are induced by the gadolinium, it is expected as seen in the figure that the magnitude of these moments decreases when the gadolinium content is reduced.

The origin of the induced moment is quite different for the nickel and for the praseodymium. In the simplest analysis the moment induced on the praseodymium is due to admixture of the crystal field states by the magnetic term $\boldsymbol{\alpha} \cdot \mathbf{J}$ in the Hamiltonian (equation (2)). Since $\boldsymbol{\alpha}$ is entirely due to the field created by the gadolinium at the site of the $Pr^{3+}$ ion it is expected to see the moment of the praseodymium vanish for zero gadolinium content. However other indirect causes including variation in the crystal field parameters or local distortions that change the site symmetry of the lanthanide ion may not have a negligible effect. A lowering of the lanthanide site symmetry will of course introduce more terms in the crystal field Hamiltonian. The moment induced on the nickel is more complex. According to the data in figure 6 the moment of nickel will vanish for a concentration of 35% of gadolinium (65% of praseodymium). At that concentration the average moment of gadolinium per formula unit is 2.5 $\mu_B$ whereas that of praseodymium is 1.75 $\mu_B$. According to these data, the polarization of the nickel subsystem is lost when the average 4f moment per unit formula is less than 1.5 $\mu_B$.

It is well known that the itinerant magnetism increases with a volume expansion; however, in the present case the opposite trend for the moment of nickel is observed. Therefore, the change in the volume of the cell cannot be responsible for the disappearance of the nickel's moment.

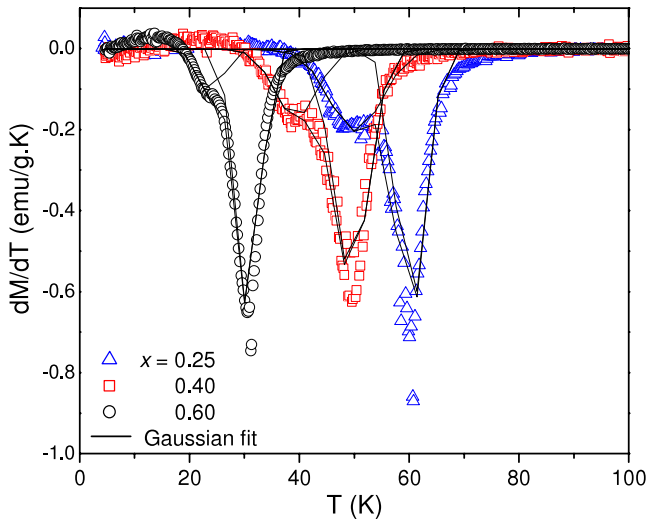


**Figure 7.** The curves $dM_{FC}(T)/dT$ at measuring field of 1 kOe for the three samples. The solid lines are the corresponding Gaussian fits.

Another factor to be considered is the increasing number and the order of the vacancies at the 4a sites with increasing praseodymium content. The existence of the vacancies allows for a relaxation of the lattice, leading to an increase of all lanthanide–lanthanide distances, a release of internal strains on the rare-earth sublattice [12] and therefore to a reduction of the hybridization. Following the results reported by Williams *et al* [23] the effect of the vacancies on the induced magnetic moments can be assessed by analysing the width of the curve $dM_{ZFC}(T)/dT$ as a function of temperature. These curves are shown in figure 7 for the three compounds. A fit of $dM/dT$ curves to a Gaussian leads to values of the average Curie temperature $\bar{T}_c$ fairly close to those determined directly from $M(T)$ plots (see table 1). The width of the line, within our uncertainty, is the same for the three compounds. Therefore it is not possible to conclude that the increasing order of the vacancies has a significant effect of the magnetic correlation or on the hybridization in this system. A quantitative estimation of the occupancy of the 4a sites and their relative ordering in either the stoichiometric or the non-stoichiometric parent sample $GdNi_2$ as well as Pr-substituted $GdNi_2$ alloys are needed to clarify the role of the vacancies in the itinerant magnetism.

## 5. Conclusion

The crystal structure and the 3d magnetism of nickel and 4f magnetism of praseodymium in the polycrystalline $Gd_{1-x}Pr_xNi_2$ series have been investigated. The results show that the whole series crystallize in the superstructure C15 exhibiting a unit cell volume expansion upon substitution of gadolinium by praseodymium. The experimental magnetic properties were analysed on the light of Weiss mean-field theory. It is found that the gadolinium induces a moment on the nickel and on the praseodymium. Moreover, the induced moments couple antiparallel to the gadolinium moment. A threshold in the concentration of gadolinium is observed below which the magnetic moment of nickel disappears.

## Acknowledgments

The authors would like to thank Dr M A H McCausland for providing the starting materials and making the sample preparation facilities available, and Professor P de Groot and G J Bowden for useful discussions. The authors are also indebted to Dr I Al-Omari for providing ASTM data and to Dr Y Hamam and Professor M Lataifeh for bringing this interesting system to their attention.

## References

[1] Buschow K H J 1980 *Ferromagnetic Materials* vol 1, ed E P Wohlfarth (Amsterdam: North-Holland) chapter 4
[2] McCausland M A H and Mackenzie I S 1980 *Nuclear Magnetic Resonance in Rare Earth Metals* (London: Taylor and Francis)
[3] Yano K, Umehara I, Miyazawa T, Adachi Y and Sato K 2005 *Physica* B **367** 81
[4] Mizumaki M, Yano K, Umehara I, Ishikawa F, Sato K, Koizumi A, Sakai N and Muro T 2003 *Phys. Rev.* B **67** 132404
[5] Nait Saada A 1980 *PhD Thesis* Université Scientifique et Médicale et l'Institut National Polytechnique de Grenoble
[6] Taylor K N R 1971 *Adv. Phys.* **20** 603
[7] Mizumaki M, Yano K, Umehara I, Ishikawa F, Sato K, Koizumi A, Sakai N and Muro T 2003 *Phys. Rev.* B **67** 132404
[8] Yano K, Tanaka Y, Matsumoto I, Umehara I, Sato K, Adachi H and Kawata H 2006 *J. Phys.: Condens. Matter* **18** 6891
[9] Mallik R, Paulose P L, Sampathkumaran E V, Patil S and Nagarajan V 1997 *Phys. Rev.* B **55** 8369
[10] Paulose P L, Patil S, Mallik R, Sampathkumaran E V and Nagarajan V 1996 *Physica* B **223/224** 382
[11] Baranov N V, Proshkin A V, Gerasimov E G, Podlesnyak A and Mesot J 2007 *Phys. Rev.* B **75** 092402
[12] Gratz E, Kottar A, Lindbaum A, Mantler M, Latroche M, Paul-Boncour V, Acet M, Barner Cl, Holzapfel W B, Pacheco V and Yvon K 1996 *J. Phys.: Condens. Matter* **8** 8351
[13] Lindbaum A, Gratz E and Heathman S 2002 *Phys. Rev.* B **65** 134114
[14] Melero J J, Burriel R and Ibarra M R 1995 *J. Magn. Magn. Mater.* **140–144** 841–2
[15] Kawatra M P, Skalski S, Mydosh J A and Budnick J L 1969 *Phys. Rev. Lett.* **23** 83
[16] Mori H, Satoh T, Fujita T and Ohtsuka T 1982 *J. Low Temp. Phys.* **49** 397
[17] Lea K R, Leask J M and Wolf W P 1962 *J. Phys. Chem. Solids* **23** 1381
[18] McMorrow D F, McCausland M A H, Han Z-P and Abel J S 1989 *J. Phys.: Condens. Matter* **1** 10439
[19] Melero J J, Burriel R and Ibarra M R 1995 *J. Magn. Magn. Mater.* **140–144** 841
[20] Latroche M, Paul-Boncour V and Percheron-Guegan A 1993 *Z. Phys. Chem.* **179** 261
[21] Nam D N H, Jonason K, Nordblad P, Khiem N V and Phuc N X 1999 *Phys. Rev.* B **59** 4189
[22] Givord D and Courtois D 1999 *J. Magn. Magn. Mater.* **196/197** 684
[23] Williams D S, Shand P M, Pekarek T M, Skomski R, Petkov V and Leslie-Pelecky D L 2003 *Phys. Rev.* B **68** 214404